

The visible spectroscopy of iron oxide minerals in dust particles from ice cores on the Tibetan Plateau

By GUANGJIAN WU^{1,2*}, TIANLI XU^{1,3}, XUELEI ZHANG⁴, CHENGLONG ZHANG⁵ and NI YAN^{1,3}, ¹Key Laboratory of Tibetan Environment Changes and Land Surface Processes, Institute of Tibetan Plateau Research, Chinese Academy of Sciences, Beijing 100101, China; ²CAS Center for Excellence in Tibetan Plateau Earth Sciences, Beijing 100101, China; ³University of Chinese Academy of Sciences, Beijing 100049, China; ⁴Northeast Institute of Geography and Agroecology, Chinese Academy of Sciences, Changchun 130102, China; ⁵Research Center for Eco-Environmental Sciences, Chinese Academy of Sciences, Beijing, 100085, China

(Manuscript received 19 July 2015; in final form 3 February 2016)

ABSTRACT

Goethite (Gt) and hematite (Hm) are the most abundant forms of iron oxides in dust and the major light absorbers in the shortwave spectrum in air and snow. Diffuse reflectance spectrometry was performed to investigate the reflectance spectra of goethite and hematite in dust particles from ice cores, aerosol samples and glacier cryoconite on the northern and central Tibetan Plateau. The results showed that two peaks in the first derivative value of the spectra at 430 and 560 nm were determined to be goethite and hematite, respectively. The high iron content samples have a higher first derivative value, and prominent and much more distinct peaks for Hm and Gt. We propose that the strength of the Hm and Gt peaks may probe the iron content, and then in our samples hematite has a stronger correlation than goethite. However, when the iron content reaches a threshold, the iron oxides have little or no impact on the reflectance spectra. The fine fraction of glacier dust has a greater abundance of iron, and the first derivative values of hematite are higher than goethite, indicating that hematite might be concentrated in the fine fraction. The distinguishable differences in the Hm/Gt ratio among these ice core samples and other aerosol data indicate the regional to continental difference in composition, which can be used to simplify the iron oxides in snow radiation models.

Keywords: ice core dust, diffuse reflectance spectroscopy, hematite, goethite, Tibetan Plateau

1. Introduction

Mineral dust is an important component of atmospheric aerosols, which can have an impact on global climate by means of radiative forcing (e.g. Sokolik and Toon, 1999) and nutrient supply to the biosphere (e.g. Jickells et al., 2005). Iron oxide minerals are efficient light scattering and absorption materials which can enhance absorption at UV and visible wavelengths (Zhang et al., 2015). The single scattering albedo (SSA) of the mixture decreases with increased hematite at solar wavelengths, while it generally increases at most IR wavelengths (Sokolik and Toon, 1999; Linke et al., 2006). The results showed that the aerosol SSA is much lower at 405 nm than at 870 nm and that SSA is

dominated by and linearly correlated with the iron content of the entrained mineral dust (Moosmuller et al., 2012). Iron oxide particles in the atmosphere play an important role in atmospheric radiative balance (Arimoto et al., 2002; Mishra and Tripathi, 2008). The light absorption by mineral dust in snow is thought to be due to iron oxides (Wang et al., 2013).

A recent Himalayan study in Nepal indicates that the effect of dust on snow albedo and radiative forcing can be considerably greater than black carbon when the impurity concentration is low (Kaspari et al., 2014). In northern China, black carbon and organic carbon dominate snow absorption and the Fe oxides contribute <10 % to the total absorption (Wang et al., 2013). Addressing this discrepancy requires detailed information about the elemental and mineralogical composition of the dust. Dust from desert regions typically contains a mixture of several Fe-bearing minerals. Iron oxides, primarily hematite and goethite, in

*Corresponding author.
email: wugj@itpcas.ac.cn

eoian dust are of wide interest in climatic, environmental and biogeochemical studies. Goethite and hematite are the most abundant forms of iron oxides in dust (Lafon et al., 2006) and the major light absorbers in the shortwave spectrum (Zhang et al., 2015). Diffuse reflectance spectrometry (DRS) is a widely used technology to discern hematite (Fe_2O_3 , Hm) and goethite (FeOOH , Gt) in a variety of sediments, such as eolian loess deposits (Ji et al., 2002), aerosols (Arimoto et al., 2002; Lafon et al., 2006; Shen et al., 2006; Formenti et al., 2008; Lazaro et al., 2008) and deep-sea sediments (Balsam and Deaton, 1991). The detection limit of DRS for hematite and goethite can be as low as 0.01 % (Balsam et al., 2014), which is advantageous for analysis of aerosol samples with low dust (iron) concentration.

Few studies have specifically investigated the iron oxide mineral particles in snow and ice. Snow albedo influences the mass balance of glaciers and the timing and volume of snow melt and runoff. Albedo of snow decreases with increasing concentrations of particulate matter near the surface. The iron oxides have a significant impact on snow/glacier albedo because iron oxides dominate light absorption by mineral dust and consequently decrease glacial melting and water resources (Kaspari et al., 2014). Glaciers are widely distributed throughout the Tibetan Plateau and serve as a special media to capture and preserve the mid- and high-tropospheric Asian dust which can be transported over great distances to the North Pacific. Therefore, it is convenient to study the long-range transported Asian dust via glacial dust. To our knowledge, laser-light scattering measurements of ice cores have been carried out to determine dust concentration (Stolz and Ram, 2005), whereas the application of DRS technology to insoluble particles in the Tibetan Plateau ice

core has not been reported. In this paper, we investigate the iron content and spectral properties of iron oxide (hematite and goethite) dust particles from ice cores on the Tibetan Plateau. Aerosol samples from the Eastern Pamirs and cryoconite on Qiyi Glacier were also analysed for comparison with the ice core dust. The main purpose of this work is to determine the relationship between observed optical properties and the concentrations of iron oxide, providing basic data for the future study of the effect of iron oxide minerals on solar radiation, snow albedo and nutrient supply.

2. Sampling and methods

2.1. Sample collection

Over the past decade, we have recovered dozens of ice cores from the Tibetan Plateau. Samples in this study include dust particles in ice cores from Muztagata Glacier (38.28°N, 75.01°E, 6250 m), Puruogangri ice cap (33.92°N, 89.01°E, 6072 m), Qiangtang No. 1 Glacier (33.17°N, 88.04°E, 5890 m) and Zangsegangri (34.32°N, 85.83°E, 6070 m) Glacier (Fig. 1). Ice was randomly selected at different depths from Puruogangri and Zangsegangri ice cores (with a thickness of 15 and 20 cm, respectively), and continuous sections from the Muztagata (31.9–39.9 m, with intervals of 100 cm) and Qiangtang No. 1 (1.30–17.02 m, with intervals of 30–49 cm) ice cores were used for the analysis. The external part of each core section was scraped away using a stainless-steel scalpel in a class 1000 clean room (at -15°C condition), and only the inner part of the cores was used for DRS and geochemical analysis (Wu et al., 2009). They were melted at room temperature in a class 1000 clean room

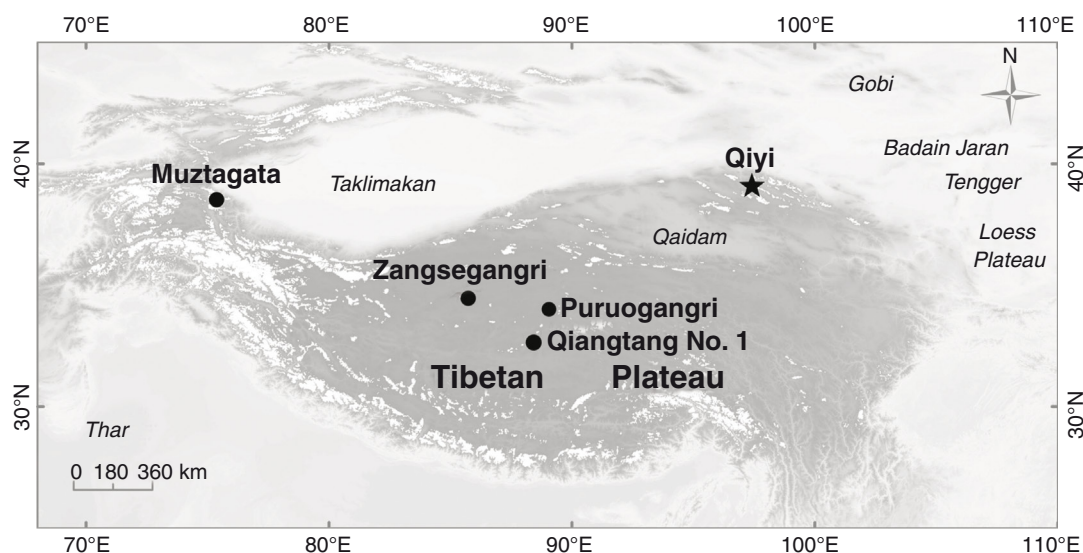


Fig. 1. Location of ice cores on the Tibetan Plateau. Dot means ice core, while star means surface snow.

and were then filtrated on an FHLC PTFE membrane (Millipore Corporation, with a diameter of 47 mm and pore size of 0.45 μm).

To make a comparison with the ice core dust, aerosol samples were collected at 10 or 15 d intervals with TefloTM membrane (Pall Corporation, with a diameter of 47 mm and pore size of 1 μm) at Mt. Muztagata (38.28°N, 75.01°E, 4430 m), located far away from cities and human activities; so aerosols collected at this site are mainly from natural sources (Wu et al., 2009). Aerosol samples collected from 30 June to 2 October 2011 were used for analysis and comparison.

The Qiyi Glacier (Chinese Glacier Inventory No. 5Y43 7C18, 39.23°N, 97.76°E) is located in the western part of Qilian Shan. A total of seven cryoconite (silt pellets) samples were collected at different altitudes (from 4442 m to 4767 m a.s.l.) on the surface of Qiyi Glacier (39.23°N, 97.75°E) in 2009 and kept frozen for experimental analysis. Particle size sorting was performed by Stokes sedimentation equation for the cryoconite (Wu et al., 2015). Then the bulk and the fine fractions (<20 μm) were analysed for their elemental composition and spectrometry to reveal the possible size effect on the DRS results.

2.2. DRS measurement

DRS is a rapid, non-destructive and low detection limit technique that provides reflectance and absorption information about the tested substance. The Muztagata (aerosol and ice core), Puruogangri, Zangsegangri and Qiangtang filter samples were analysed using a TU 1901 double beam UV-V Spectrophotometer (Puxi General Instrumental Company, China). For the Qiyi cryoconite (bulk and fine fractions), dust particles (more than 2 g for the bulk, while 0.36–0.75 g for the fine fraction, to ensure they were completely opaque in the sample container) were fixed on the board with glue and then measured using the TU 1901. Filters were scanned from 300 to 850 nm at 1-nm intervals, including near ultraviolet, visible and near infrared. The instruments were calibrated before detection using a standard white board (barium sulphate), and the experiment carried out when the error was below 1%. The data from the visible wavelength (400–700 nm) are discussed in this paper.

The reflectance spectrum of these samples is relatively flat, so researchers always use the first derivative curves to denote the mineral component (Balsam and Deaton, 1991). The first derivative of DRS curves is thought to be the best method currently available for qualitatively detecting the mineral hematite at the low concentrations found in soils, sediments and rocks (Balsam et al., 2014). In this study, the first derivative of the reflectance spectra is also used, which shows many wave peaks denoting certain characteristic mineral components, such as the iron oxides.

Here we calculate the first derivative at intervals of 9 nm, as in the following formula:

$$D_{n+5} = (R_{n+9} - R_n)/9,$$

where D_{n+5} is the first derivative value of reflectance spectra at wavelength $n+5$; R_{n+9} and R_n reflectance spectra at wavelength $n+9$ and n , respectively. After calculation, the first derivative values in this study were smoothed with 15 points following Scheinost et al. (1998), which seems to be the optimum number of points to obtain smooth curves.

2.3. Dust iron content measurement

After DRS measuring and weighting, the ice core dust filters, aerosol filters and cryoconite were dissolved with ultra-pure HNO_3 –HF at 150–190 °C in PTFE screw-top bombs. After digestion, the dust on the filters was completely dissolved. Quantitative elemental analyses of the samples were performed using inductively coupled plasma-mass spectrometry (ICP–MS, Thermo X-7, Thermo-Elemental Corporation). The digestion and measurement processes, and detection limit and precision of ICP–MS have been described in detail previously (Wu et al., 2009). Due to the high concentration of the cryoconite, the major elements, including Fe, were measured using inductively coupled plasma optical emission spectrometry (ICP–OES, Leeman Labs Prodigy-H).

3. Results and discussion

3.1. Iron abundance in ice core dust

A previous study has revealed that the abundance of iron in ice core dust differs along the north-south transect of High Asia (Wu et al., 2012). In this study, new data from four ice cores in the central and western Tibetan Plateau are presented (Table 1). The ice core dust from the central and inner Tibetan Plateau show similar amounts of iron, with 3.87 % at Zangsegangri and 3.23 % at Puruogangri, with the Qiangtang ice core dust showing greater abundance of iron at 4.32 %. At Muztagata, iron abundance is identical in the ice core dust and aerosol samples, with an average of 4.06 %. The difference is not obvious, but distinguishable, providing a detailed and accurate description of the geochemical composition of these ice core dusts. The data reveal that even for the Asian dust, differences in iron abundance have been revealed on a regional scale.

The global average iron level in the upper continental crust is 3.5 % (Taylor and McLennan, 1985), which is widely accepted as the iron content of atmospheric dust. However, there is great variation in this value on the regional to continental scale (Shi et al., 2012). Dust in the Sahelian region is characterised by a high Fe/Al ratio due to

Table 1. The averaged iron abundance (analysed by ICP-MS) and first derivative value (at 9-nm interval and after 15-point smoothing) of goethite (Gt), hematite (Hm) and the Hm/Gt ratios of the dust from Tibetan Plateau ice core, and comparison with atmospheric aerosols from northern China and West Africa

Location	Fe % (SD)	Averaged Gt	averaged Hm	Hm/Gt (SD)	Reference
Muztagata, ice core	4.06 (1.04)	0.20	0.13	0.67 (0.14)	this study
Qiangtang No. 1, ice core	4.32 (1.21)	0.16	0.12	0.72 (0.22)	this study
Zangsegangri, ice core	3.87 (1.35)	0.12	0.10	0.80 (0.40)	this study
Puruogangri, ice core	3.23 (1.46)	0.11	0.07	0.55 (0.28)	this study
Muztagata, aerosol	4.07 (1.02)	0.13	0.09	0.69 (0.21)	this study
Qiyi, cryoconite (bulk)	4.48 (0.18)	0.18	0.16	0.89 (0.04)	this study
Qiyi, cryoconite (fine)	5.36 (0.09)	0.19	0.19	0.99 (0.03)	this study
Yulin, aerosol				0.59 (0.16)	Shen et al., 2006
Dunhuang, aerosol				0.57 (0.26)	Shen et al., 2006
Tongliao, aerosol				0.46 (0.13)	Shen et al., 2006
North Atlantic, aerosol				0.93 (0.23)	Arimoto et al., 2002
Canary Island, aerosol				1.01 (0.47)	Lazaro et al., 2008
West Africa, aerosol				^a 0.62 (0.19)	Formenti et al., 2014

^aApparent fraction of Fe by X-ray absorption near edge structure (XANES).

the abundance of ferralitic soils there, with a Fe content of 5.7 % (Shi et al., 2011). In contrast, soils in the semi-arid regions of central Asia contain less Fe (Sokolik and Toon, 1999), indicating there are regional differences in iron abundance.

3.2. The reflectance and the first derivative curves

The reflectance spectra of standard white board (baseline, 100 % reflectance in theory), blank filters (Millipore Corporation FHLC PTFE, and Pall Corporation Teflo) and typical samples are shown in Fig. 2. Our results show that blank filters (FHLC PTFE for ice core dust and Teflo

for aerosol) are absorbent to light, while the first derivative of the reflectance spectra of a blank filter is smooth, without peaks indicative of iron oxide minerals (Fig. 3), indicating that the absorption of a blank filter does not affect the DRS peaks of iron oxide minerals. The reflectance spectrum of standard white board (barium sulphate) is consistent with the value of almost 100 %, without apparent fluctuations. The reflectance spectra of samples are obviously lower than that of standard white board and blank filters, indicating that reflection and absorption coexist in the samples analysed. The reflectance spectra show a large difference between the ice core and aerosol samples.

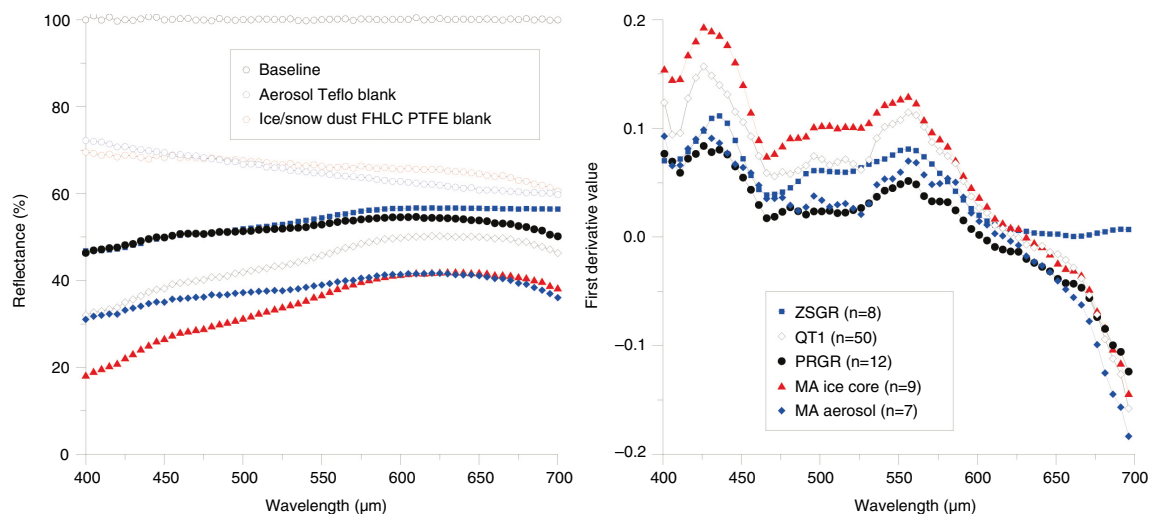


Fig. 2. The averaged reflectance (%) and first derivative value (after 15-point smoothing) of Qiantang No. 1 (QT1), Puruogangri (PRGR), Zangsegangri (ZSGR), Muztagata (MA ice core) ice core dust samples, and Muztagata aerosol (MA aerosol) samples. The result of blank filters (Teflo and PTFE) is also presented. Note that all the dots are drawn at 5-nm intervals.

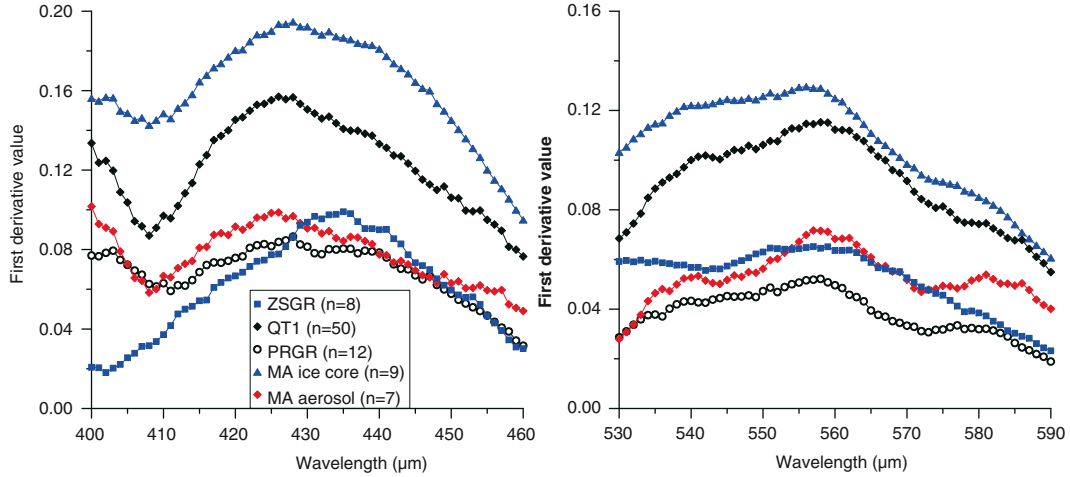


Fig. 3. The averaged first derivative values of the ice core and aerosol dust samples from 400 to 460 nm and from 530 to 590 nm. Please note the two peaks appear at around 430 and 560 nm.

The first derivative of the reflectance spectra is a sensitive indicator for hematite and goethite in the visible wavelength. The peak between 555 and 575 nm indicates hematite, while goethite has two indicative peaks around 435 and 535 nm. The first derivative curves of most of the samples (dust particles in QT1 ice core, Puruogangri ice core, Muztagata ice core and aerosol collected at Muztagata) have two distinct peaks around 430 and 560 nm, which indicate the presence of goethite and hematite, respectively, showing that the Tibetan ice core dust also contains the two iron oxides. These two characteristic peaks are essentially the same as those reported previously in African and Asian aerosols (e.g. Arimoto et al., 2002; Shen et al., 2006; Lazaro et al., 2008). The peak value of goethite is slightly higher than hematite, suggesting that goethite contributes more to total iron minerals in Tibetan ice core dust, as pointed out in previous studies (e.g. Ji et al., 2002).

We then checked the exact position of the characteristic peaks for hematite and goethite in ice core dust. All of the samples showed the same hematite peak at 558 nm. Although some studies have shown that the characteristic peak for hematite can range from 555 nm at low concentrations to 575 nm at high concentrations (Arimoto et al., 2002), our ice core dust samples, containing a different iron content, displayed a stable hematite peak position. All of the ice core and aerosol dust showed the same goethite peak at ~ 428 nm wavelength in the first derivative curve, except for Zangsegangri, whose peak appears at 435 nm. Jiang et al. (2013) reported that the aluminium (Al) substitution for goethite in Chinese loess samples can significantly influence the peak positions and amplitudes of the goethite DRS band. Whether this is the cause for the change of position of goethite for Zangsegangri dust needs further study.

3.3. The effect of iron content on the first derivative curves

The value of the first derivative peaks is related to the content of hematite and goethite (Balsam et al., 2014). For some samples with very low dust concentrations, the indicative peaks are weak or not found, especially for hematite (Fig. 4). This phenomenon may be related to low iron content in the samples. In order to check the impact of iron content on the reflectance spectra of dust samples, we grouped all samples into three types (low, middle and high) according to iron content (measured by ICP-MS). Here we need to point out that the standard of low, middle and high iron concentration is defined relative to each site. Since dust particles are supposed to be uniformly distributed on the membrane filter during filtration and aerosol collection, in this study we use the iron mass on the filter to represent the iron content.

The first derivative value for each sample is shown in different colours according to iron concentration (Fig. 4). At Qiangtang, Puruogangri and Zangsegangri, the low concentration samples (grey lines) have a low first derivative value and weak characteristic peaks for goethite and hematite. The middle concentration samples (blue lines) show a higher first derivative value and stronger characteristic peaks. The high concentration samples (red lines) have the highest first derivative value, and the characteristic peaks of goethite and hematite are much more distinct and prominent than the low and middle concentration samples. Although this trend was not demonstrated in the Muztagata ice core dust, it was found in the QT1 ice core and the Muztagata aerosol sample (not shown). Therefore, iron content can have a direct impact on the reflectance spectra of Tibetan ice core dust.

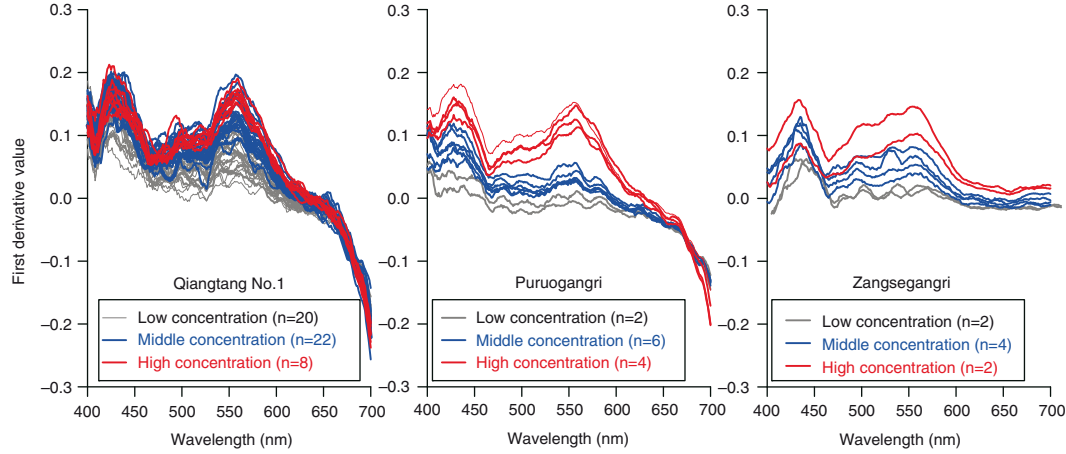


Fig. 4. The first derivative curve of each dust sample in Qiangtang, Puruogangri and Zangsegangri ice cores with different iron concentrations. Note that the standard of low, middle and high iron concentration is defined relative to each site.

We then tested the correlation between iron content and the strength of the characteristic peaks for goethite and hematite. In the Puruogangri and QT1 ice core, both hematite and goethite showed a positive correlation with iron content, and the indicative goethite and hematite peaks in the first derivative curves became apparent as iron content increased. This correlation was much stronger (with greater R^2) for hematite than goethite, indicating that hematite has a greater impact on reflectance at the wavelength 558 nm than goethite at 428 nm since hematite has a relative higher complex refractive index and lower calculated SSA (Zhang et al., 2015). Our result gives the regression correlation between iron content and the first derivative value peak of hematite and goethite, supporting the correlation reported in studies of African (Arimoto et al., 2002) and Asian (Shen et al., 2006) dust aerosols. However, the Muztagata and Puruogangri ice core dust did not show such a trend. Possible reasons include the small number of samples at each of the sites, and different dust sources and composition. Although the ICP-MS and DRS can respectively determine total iron abundance and the relative Hm and Gt content, the detailed iron fraction (iron oxides and other iron-containing minerals) is not known and needs further investigation.

In Fig. 5, the strength of the first derivative value for hematite (goethite) increases rapidly when the iron content increases slightly and is less than $500 \mu\text{g}$ per filter, or $\sim 29 \mu\text{g cm}^{-2}$ (filter diameter = 47 mm). When the iron content reaches the threshold of $\sim 500 \mu\text{g}$ per filter, the first derivative strength of the characteristic peak seems to stabilise, or even decrease slightly. This non-linear relationship between iron content and first derivative value has two possible explanations. Some researchers argue that the Fe-containing minerals, instead of the iron oxides, such as clays, can contribute to high iron content but have little

effect on the dust's reflectance spectra (Balsam and Damuth, 2000; Shen et al., 2006). An alternative explanation is that there is a threshold in iron content which can have an impact on the DRS results. If we assume the iron oxide particles are of a stable percentage in the dust, then increases in dust would also result in higher iron oxide content, and not just the addition of other Fe-containing minerals. Our results indicate that once the dust (iron oxide) content reaches a certain threshold, its impact on reflectance might stabilise. This in turn highlights the radiative influence of iron oxides in atmospheric dust, despite the low content.

3.4. The effect of particle size on the first derivative of reflectance spectra

The effect of the size of an atmospheric dust particle on its reflectance is not clear. Due to the small amount of dust in ice core samples, it is not realistic to separate the coarse and fine fractions. Here, we take the cryoconite, the aggregated eolian dust particles combined with biogenic materials, on the glacier surface to evaluate the possible effect. Cryoconite samples were collected from different altitudes on the Qiyi glacier surface, and then the fine fraction ($< 20 \mu\text{m}$) was extracted to make a comparison with the bulk. The DRS results for the fine and bulk fractions are shown in Fig. 6.

The first derivative curves for the fine and bulk fractions are presented in Fig. 6. The reflectance percentage of fine particles is higher than the bulk fraction. The iron abundance is greater in the fine fraction (5.36 %) than in the bulk (4.48 %). The differences in iron content and the consequent DRS results are attributed to the particle grain size sorting. Small particles have a larger surface area to volume ratio than coarse particles and consequently possess increased scattering efficiency. The smaller the particle size, the greater the reflectivity. Previous experiments have indicated that

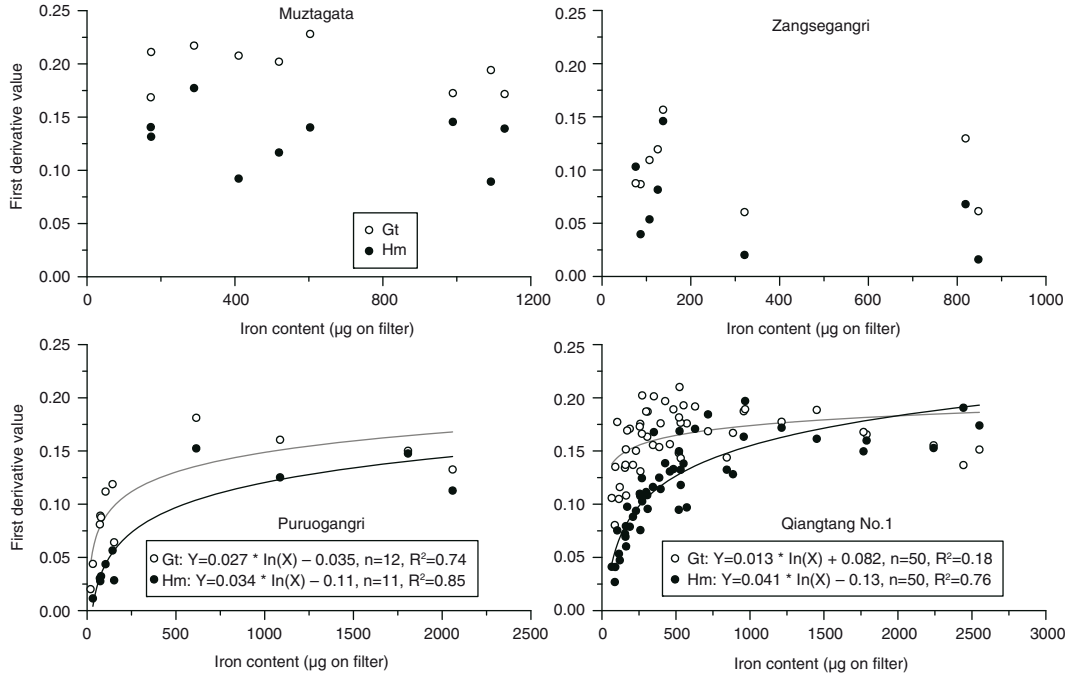


Fig. 5. The correlation between iron content (mass on the filter) and the first derivative value of goethite (Gt) and hematite (Hm) in Tibetan ice core dust.

particle size plays an important role in reflectance characteristics, and that reflectance increases with a decrease in particle size (Bhargava and Mariam, 1991). Further, the hematite peak has a greater first derivative value than that of goethite in the fine fraction, indicating that hematite might be concentrated in the fine dust particles, as pointed out in previous research reporting a possible enrichment of hematite in the fine aerosol fraction (Linke et al., 2006).

The goethite peak position changed slightly in the bulk fraction. Both the bulk and fine fractions have an identical hematite peak at 555 nm in the first derivative value.

For the goethite peak, a difference between the bulk and fine fractions exists. In the fine fraction, only one peak appears at 425 nm for goethite. The bulk sample shows two peaks for goethite, a weak one at 425 and a prominent one at 478 nm. It has been reported that the position of the characteristic peak might change depending on iron oxide concentration (Arimoto et al., 2002). Our findings suggest that grain size could also change the peak position.

There is a variation in the first derivative of reflectance spectra for bulk samples between 640 and 700 nm wavelength, which is different from that of the fine samples that

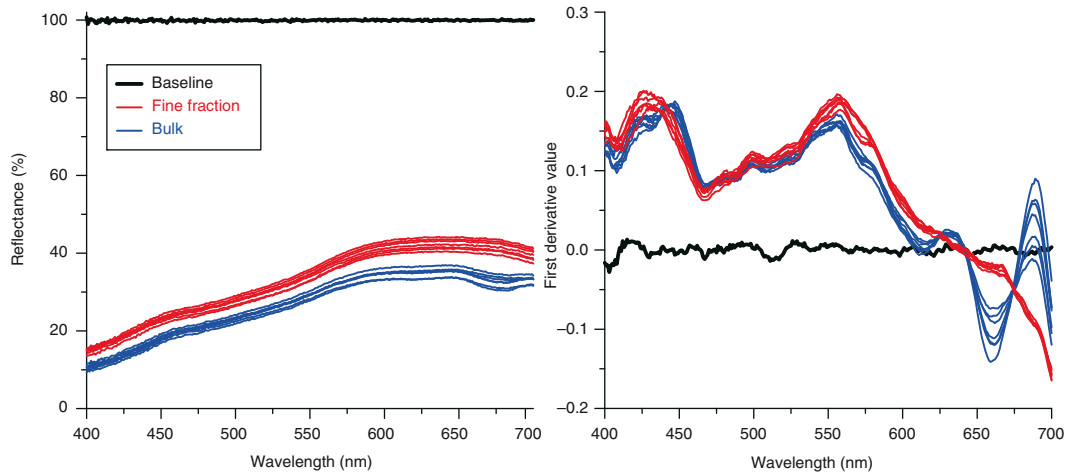


Fig. 6. Reflectance percentage and first derivative curve of the fine and bulk fractions of Qiyi cryoconite.

decreases gradually. We attribute this difference to the change of particle size, which can impact the DRS by the grain size distribution and by the size sorting (which can change the iron content) between the bulk and the fine fractions.

3.5. Ratio of hematite to goethite and regional differences in dust revealed by DRS

Reflectance spectroscopy can be used to quantify the ratio of hematite to goethite in a particular dust sample. Iron is the primary light-absorbing constituent in mineral dust, with the spectral absorption characteristics of the dust dependent on the form of the iron oxide (Sokolik and Toon, 1999; Lafon et al., 2006). Hematite and goethite have different complex refractive indices (Zhang et al., 2015) and their partitioning is relevant to the direct effect of mineral dust on radiation in the shortwave spectrum (Formenti et al., 2014). Therefore knowledge of their content can aid in better understanding of the radiative properties of dust. The ratio of hematite to goethite (Hm/Gt) in dust is used as an indicator of the relative proportions of hematite and goethite in eolian dusts.

In this study, we calculated the value of the Hm/Gt ratio according to the values of goethite and hematite on the first derivative curves. Among the sites studied, the ratio varied from 0.53 (Puruogangri) to 0.80 (Zangsegangri). The Muztagata ice core dust has the same ratio as the aerosol, indicating that they have the same source, as shown by the element composition (Wu et al., 2015). The Hm/Gt ratio of Tibetan ice core dust (0.68) is a little higher than that of the aerosol dust over northern China (0.54, Shen et al., 2006). This might result from the different types of dust (aerosol vs. ice core dust) and/or the different dust sources. The potential dust source regions for these ice cores differ. Taklimakan desert is the main source for Qiyi Glacier dust (Wu et al., 2010, 2015). Zangsegangri, Puruogangri, and Qiangtang No. 1 glaciers are located in the central Tibetan Plateau, where local dust also contributes to the dust aerosols (Zhang et al., 1996). The dust sources of Muztagata are mainly west Asian, central Asian and Taklimakan (Wu et al., 2009). Although accurate provenance tracing (e.g. Sr and Nd isotope) for our ice core dust is not available at present, regional differences in the Hm/Gt ratio are distinguishable and indicate that iron oxide varies on a regional scale.

The continental (Asian vs. African) difference in the Hm/Gt ratio is clear. African dust contains more hematite and has a higher Hm/Gt ratio (Arimoto et al., 2002), while Asian dust has a relatively low Hm/Gt ratio (Shen et al., 2006). The iron in Asian dust is most often found in the

form of goethite (Ji et al., 2002; Lafon et al., 2006), which has been assumed to be the representative of iron oxide and has been used to calculate the light absorption in northern China snow (Wang et al., 2013). Some researchers argue that the Hm/Gt ratio of dust also depends on the nature and history of the source soils (Lazaro et al., 2008; Shi et al., 2011), and goethite dominates in West African dust (Formenti et al., 2014). Dust deposited in snow cover in the Wasatch Range (Utah, USA) indicates roughly equal amounts of hematite and goethite, while goethite is the dominant ferric oxide and seems to be the main iron oxide control on the absorption of solar radiation (Reynolds et al., 2014). Although some radiative models suppose that iron oxides can be represented by only one mineralogical species, that is, hematite, it is still necessary to quantify the proportion of hematite and goethite, the two major iron oxide species in mineral dust (Formenti et al., 2014). Therefore, detailed information about hematite and goethite in these types of dust can contribute to a comprehensive understanding of their composition and climatic effects.

4. Conclusion

In this study, we reported the diffuse reflectance spectroscopic measurements of dust from ice cores, aerosol samples and cryoconite from the Tibetan Plateau and provided information on the iron oxides of mid- to high-troposphere Asian dust. The DRS analysis finds that both goethite and hematite exist in Tibetan ice core dust, with characteristic peaks at 430 and 560 nm, respectively in the first derivative curve of reflectance. The first derivative curves are affected by the iron content of dust particles. The more prominent peaks with very distinct characteristics appear correlated with the iron content. Although a calibration is missing, a quantitative correlation between them is proposed. The strength of the goethite and hematite peaks increases with iron content, and the former has a stronger correlation than the latter. However, when the iron content reaches a threshold, its impact on reflectance seems to stabilise.

DRS of the bulk and fine fractions of cryoconite indicates that particle size has an impact on the reflectance spectra of dust, even with the same elemental composition. The reflectance is relatively higher with a fine particle size. The Hm/Gt ratios of the samples show a remarkable difference in the continental and regional scales. Tibetan ice core dust has a slightly higher Hm/Gt ratio than the aerosol dust over northern China. Compared to African aerosols, Asian dust has a relatively lower Hm/Gt ratio, indicating that goethite dominates. The Hm/Gt ratio can be used to simplify the proportion of iron oxides in the radiative forcing models.

5. Acknowledgements

We are grateful to team members for the ice core drilling and Caroline Brimblecombe for improving the text. This work is supported by the NSFC (Grant No. 41271074, 41190083) and CAS Strategic Priority Research Program B (Grant No. XDB03030101).

References

- Arimoto, R., Balsam, W. and Schloesslin, C. 2002. Visible spectroscopy of aerosol particles collected on filter: iron-oxide minerals. *Atmos. Environ.* **36**(1), 89–96. DOI: [http://dx.doi.org/10.1016/S1352-2310\(01\)00465-4](http://dx.doi.org/10.1016/S1352-2310(01)00465-4)
- Balsam, W., Ji, J., Renock, D., Deaton, B. C. and Williams, E. 2014. Determining hematite content from NUV/Vis/NIR spectra: limits of detection. *Am. Mineral.* **99**(11–12), 2280–2291. DOI: <http://dx.doi.org/10.2138/am-2014-4878>
- Balsam, W. L. and Damuth, J. E. 2000. Further investigations of shipboard vs. shore-based spectral data: implications for interpreting Leg 164 sediment composition. In: *Proceedings ODP Scientific Results* (eds. C. K. Paull, R. Matsumoto, P. J. Wallace, W. P. Dillon) Vol. 164, Ocean Drilling Program, Texas A&M University, Texas, TX, pp. 313–324.
- Balsam, W. L. and Deaton, B. C. 1991. Sediment dispersal in the Atlantic Ocean: evaluation by visible light spectra. *Rev. Aquat. Sci.* **4**, 411–447.
- Bhargava, D. and Mariam, D. W. 1991. Effects of suspended particle size and concentration on reflectance measurements. *Photogramm. Eng. Rem. S.* **57**(5), 519–529. DOI: <http://dx.doi.org/10.1007/BF02999210>
- Formenti, P., Caquineau, S., Chevaillier, S., Klaver, A., Desboeufs, K. and co-authors. 2014. Dominance of goethite over hematite in iron oxides of mineral dust from Western Africa: quantitative partitioning by X-ray absorption spectroscopy. *J. Geophys. Res. Atmos.* **119**, 12740–12754. DOI: <http://dx.doi.org/10.1002/2014JD021668>
- Formenti, P., Rajot, J. L., Desboeufs, K., Caquineau, S., Chevaillier, S. and co-authors. 2008. Regional variability of the composition of mineral dust from western Africa: Results from the AMMA SOP0/DABEX and DODO field campaigns *J. Geophys. Res.* **113**, D00C13, DOI: <http://dx.doi.org/10.1029/2008jd009903>
- Ji, J. F., Balsam, W. L., Chen, J. and Liu, L. W. 2002. Rapid and quantitative measurement of hematite and goethite in the Chinese loess-paleosol sequences by diffuse reflectance spectroscopy. *Clay Clay Miner.* **50**, 208–216.
- Jiang, Z. X., Liu, Q. S., Colombo, C., Barron, V. and Torrent, J. 2013. Quantification of Al-goethite from diffuse reflectance spectroscopy and magnetic methods. *Geophys. J. Int.* **196**, 131–144. DOI: <http://dx.doi.org/10.1093/gji/ggt377>
- Jickells, T. D., An, Z., Andersen, K. K., Baker, A. R., Bergametti, G. and co-authors. 2005. Global iron connections between desert dust, ocean biogeochemistry, and climate. *Science*. **308**, 67–71. DOI: <http://dx.doi.org/10.1126/science.1105959>
- Kaspari, S., Painter, T., Gysel, M., Skiles, S. and Schwikowski, M. 2014. Seasonal and elevational variations of black carbon and dust in snow and ice in the Solu-Khumbu, Nepal and estimated radiative forcings. *Atmos. Chem. Phys.* **14**, 8089–8103. DOI: <http://dx.doi.org/10.5194/acp-14-8089-2014>
- Lafon, S., Sokolik, I. N., Rajot, J. L., Caquineau, S. and Gaudichet, A. 2006. Characterization of iron oxides in mineral dust aerosols: implications for light absorption. *J. Geophys. Res.* **111**, D21207. DOI: <http://dx.doi.org/10.1029/2005JD007016>
- Lazaro, F. J., Gutierrez, L., Barron, V. and Gelado, M. D. 2008. The speciation of iron in desert dust collected in Gran Canaria (Canary Islands): combined chemical, magnetic and optical analysis. *Atmos. Environ.* **42**, 8987–8996. DOI: <http://dx.doi.org/10.1016/j.atmosenv.2008.09.035>
- Linke, C., Mohler, O., Veres, A., Mohacsi, A., Bozoki, Z. and co-authors. 2006. Optical properties and mineralogical composition of different Saharan mineral dust samples: a laboratory study. *Atmos. Chem. Phys.* **6**, 3315–3323. DOI: <http://dx.doi.org/10.5194/acp-6-3315-2006>
- Mishra, S. K. and Tripathi, S. N. 2008. Modeling optical properties of mineral dust over the Indian Desert. *J. Geophys. Res.* **113**, D23201. DOI: <http://dx.doi.org/10.1029/2008JD010048>
- Moosmuller, H., Engelbrecht, J. P., Skiba, M., Frey, G., Chakrabarty, R. K. and co-authors. 2012. Single scattering albedo of fine mineral dust aerosols controlled by iron concentration. *J. Geophys. Res.* **117**, D11210. DOI: <http://dx.doi.org/10.1029/2011JD016909>
- Reynolds, R. L., Goldstein, H. L., Moskowitz, B. M., Bryant, A. C., Skiles, S. M. and co-authors. 2014. Composition of dust deposited to snow cover in the Wasatch Range (Utah, USA): controls on radiative properties of snow cover and comparison to some dust-source sediments. *Aeolian Res.* **15**, 73–90. DOI: <http://dx.doi.org/10.1016/j.aeolia.2013.08.001>
- Scheinost, A., Chavernas, A., Barron, V. and Torrent, J. 1998. Use and limitations of second-derivative diffuse reflectance spectroscopy in the visible to near-infrared range to identify and quantify Fe oxide minerals in soils. *Clay Clay Miner.* **46**(5), 528–536. DOI: <http://dx.doi.org/10.1346/CCMN.1998.0460506>
- Shen, Z. X., Cao, J. J., Zhang, X. Y., Arimoto, R., Ji, J. F. and co-authors. 2006. Spectroscopic analysis of iron-oxide minerals in aerosol particles from northern China. *Sci. Total Environ.* **367**, 899–907. DOI: <http://dx.doi.org/10.1016/j.scitotenv.2006.01.003>
- Shi, Z., Krom, M. D., Bonneville, S., Baker, A. R., Bristow, C. and co-authors. 2011. Influence of chemical weathering and aging of iron oxides on the potential iron solubility of Saharan dust during simulated atmospheric processing. *Global Biogeochem. Cycles* **25**, GB2010. DOI: <http://dx.doi.org/10.1029/2010GB003837>
- Shi, Z., Krom, M. D., Jickells, T. D., Boneville, S., Carslaw, K. S. and co-authors. 2012. Impacts on iron solubility in the mineral dust by processes in the source region and the atmosphere: a review. *Aeolian Res.* **5**, 21–42. DOI: <http://dx.doi.org/10.1016/j.aeolia.2012.03.001>
- Sokolik, I. N. and Toon, O. B. 1999. Incorporation of mineralogical composition into models of the radiative properties of mineral aerosol from UV to IR wavelengths. *J. Geophys. Res.* **104**, 9423–9444. DOI: <http://dx.doi.org/10.1029/1998JD000048>

- Stolz, M. R. and Ram, M. 2005. Using laser-light scattering to measure impurities, bubbles, and imperfections in ice cores. *J. Geophys. Res.* **110**, D11209. DOI: <http://dx.doi.org/10.1029/2004JD005589>
- Taylor, S. R. and McLennan, S. M. 1985. The continental crust: its composition and evolution. *Rev. Geophys.* **33**, 241–265. DOI: <http://dx.doi.org/10.1029/95RG00262>
- Wang, X., Doherty, S. J. and Huang, J. 2013. Black carbon and other light-absorbing impurities in snow across Northern China. *J. Geophys. Res. Atmos.* **118**, 1471–1492. DOI: <http://dx.doi.org/10.1029/2012JD018291>
- Wu, G. J., Xu, B. Q., Zhang, C. L., Gao, S. P. and Yao, T. D. 2009. Geochemistry of dust aerosol over the Eastern Pamirs. *Geochim. Cosmochim. Acta* **73**(4), 977–989. DOI: <http://dx.doi.org/10.1016/j.gca.2008.11.022>
- Wu, G. J., Zhang, C. L., Li, Z. Q., Zhang, X. L. and Gao, S. P. 2012. Iron content and solubility in dust from high-alpine snow along a north-south transect of High Asia. *Tellus B* **64**, 17735. DOI: <http://dx.doi.org/10.3402/tellusb.v64i0.17735>
- Wu, G. J., Zhang, C. L., Zhang, X. L., Tian, L. D. and Yao, T. D. 2010. Sr and Nd isotopic composition of dust in Dunde ice core, Northern China: implications for source tracing and use as an analogue of long-range transported Asian dust. *Earth Planet. Sci. Lett.* **299**(3–4), 409–416. DOI: <http://dx.doi.org/10.1016/j.epsl.2010.09.021>
- Wu, G. J., Zhang, C. L., Zhang, X. L., Xu, T. L., Yan, N. and co-authors. 2015. The environmental implications for dust in high-alpine snow and ice cores in Asian mountains. *Global Planet. Change* **124**, 22–29. DOI: <http://dx.doi.org/10.1016/j.gloplacha.2014.11.007>
- Zhang, X. L., Wu, G. J., Zhang, C. L., Xu, T. L. and Zhou, Q. Q. 2015. What's the real role of iron-oxides in the optical properties of dust aerosols? *Atmos. Chem. Phys. Discuss.* **15**, 5619–5662. DOI: <http://dx.doi.org/10.5194/acpd-15-5619-2015>
- Zhang, X. Y., Shen, Z. B., Zhang, G. Y., Chen, T. and Liu, H. Y. 1996. Remote mineral aerosols in Westerlies and their contributions to the Chinese loess. *Sci. China (Series D)*. **39**(2), 134–143.